Statistica Sinica **24** (2014), 83-100
doi:http://dx.doi.org/10.5705/ss.2012.052

RANK-BASED TAPERING ESTIMATION OF BANDABLE CORRELATION MATRICES

Lingzhou Xue and Hui Zou

The Pennsylvania State University and University of Minnesota

Abstract: The nonparanormal model assumes that variables follow a multivariate normal distribution after a set of unknown monotone increasing transformations. It is a flexible generalization of the normal model but retains the nice interpretability of the latter. In this paper we propose a rank-based tapering estimator for estimating the correlation matrix in the nonparanormal model in which the variables have a natural order. The rank-based tapering estimator does not require knowing or estimating the monotone transformation functions. We establish the rates of convergence of the rank-based tapering under Frobenius and matrix operator norms, where the dimension is allowed to grow at a nearly exponential rate relative to the sample size. Monte Carlo simulation is used to demonstrate the finite performance of the rank-based tapering estimator. A data example is used to illustrate the nonparanormal model and the efficacy of the proposed rank-based tapering estimator.

Key words and phrases: Banding, correlation matrix, Gaussian copula, tapering, nonparanormal model, variable transformation.

1. Introduction

Estimating large covariance matrices has been a much researched topic in recent years. High-dimensional data appear in many fields, but the usual sample covariance matrix is a very poor estimator of the covariance matrix in the high-dimensional setting (Johnstone (2001)). Better covariance estimators can be produced by using regularization methods, including banding (Wu and Pourahmadi (2003), Bickel and Levina (2008a)), tapering (Furrer and Bengtsson (2007), Cai, Zhang, and Zhou (2010)) and thresholding (Bickel and Levina (2008b), El Karoui (2008), Rothman, Levina, and Zhu (2010), Cai and Liu (2011)). Thresholding achieves a good variance-bias tradeoff by truncating small entries of the sample covariance matrix to zero. Thresholding is permutation invariant. On the other hand, banding and tapering utilize the underlying bandable structure of the population covariance matrix. It has shown that banding/tapering performs better than thresholding when there is a natural order among variables and two variables become near independent as they far apart in that order

(Bickel and Levina (2008a), Cai, Zhang, and Zhou (2010), Cai and Zhou (2012), Xue and Zou (2013)).

The minimax results in Cai, Zhang, and Zhou (2010) and Cai and Zhou (2012) greatly deepen our understanding of the tapering estimator of large bandable covariance matrices. Minimax lower bounds were established for collections of multivariate normal distributions, that suggest that the covariance matrix estimation problem is not any easier with normal data. Technically, the rates of convergence of banding or tapering can be established under a weaker sub-Gaussian distribution assumption (Bickel and Levina (2008a,b), Cai, Zhang, and Zhou (2010), Cai and Zhou (2012)). Normality is important to the model interpretation, because a zero entry implies the marginal independence of a pair of variables; this does not always hold without the normality assumption. In practice, observed data are often skewed or have heavy tails, especially in the high-dimensional setting. Neither normal nor sub-Gaussian distributions can be used to model such data. It is of importance and interest to relax the normality assumption while keeping its useful interpretability.

To this end, we consider the nonparanormal model which basically uses a transformation strategy to handle non-normal data.

> **The nonparanormal model:** $(X_1, \ldots, X_p)$ *follows a nonparanormal distribution if there exists a vector of unknown univariate monotone increasing transformations, denoted by* $\boldsymbol{f} = (f_1, \cdots, f_p)$*, such that the transformed random vector follows a multivariate normal distribution with mean 0 and covariance* $\mathbf{\Sigma}$*:*
>
> $$(f_1(X_1), \cdots, f_p(X_p)) \sim N_p(0, \mathbf{\Sigma}), \tag{1.1}$$
>
> where without loss of generality we let the diagonals of $\mathbf{\Sigma}$ all equal 1.

Note that $\mathbf{\Sigma}$ is also the correlation matrix; this is useful when developing a good estimator of $\mathbf{\Sigma}$. By definition of the nonparanormal model, one can see that $\mathbf{\Sigma}_{ij} = 0$ if and only if X_i and X_j are marginally independent. Any continuous variable can be transformed to a standard normal variable via a monotone increasing transformation, so the nonparanormal model assumes that after these individual transformations the marginally normal variables have a joint normal distribution. This is the parametric part of model (1.1). The nonparanormal model is a semiparametric Gaussian copula model and copula models have generated a lot of interest in statistics, econometrics and finance (Klaassen and Wellner (1997), Song (2000), Tsukahara (2005), Chen and Fan (2006), Chen, Fan, and Tsyrennikov (2006), Song, Li, and Yuan (2009)). In the context of nonparametric graphical modeling, Liu, Lafferty, and Wasserman (2009) used model (1.1) and coined the new name "nonparanormal model". We follow their terminology in this paper.

When the nonparanormal model is applied to variables with a natural order, existing results on large covariance matrix estimation suggest the use of banding or tapering to estimate $\mathbf{\Sigma}$. However, an obvious difficulty is that the nonparanormal model has p unknown nonparametric transformation functions, and it appears that one must estimate these p transformation functions in the process of estimating $\mathbf{\Sigma}$. Still we propose a rank-based tapering estimator of $\mathbf{\Sigma}$ that does not require estimating these unknown transformation functions. Our estimator is constructed in two steps. We first construct a nonparametric rank-based sample estimate of $\mathbf{\Sigma}$. The rank-based tapering estimator is then obtained by applying tapering to the rank-based sample estimate of $\mathbf{\Sigma}$. We establish rates of convergence of the rank-based tapering estimator under both the Frobenius and matrix operator norms. It is shown that the rank-based tapering estimator is consistent even when the dimension is nearly exponentially large relative to the sample size.

The rest of the paper is organized as follows. Section 2 contains the methodological details of the rank-based tapering estimator. In Section 3 we present the main theoretical results. In Section 4 we use Monte Carlo simulation to demonstrate the good finite sample performance of the rank-based tapering estimator. Rock spectrum data are used to illustrate the nonparanormal model and the efficacy of the rank-based tapering estimator. Proofs are presented in the appendix.

2. Methodology

Throughout the paper, we assume that we have n identically independently distributed (*i.i.d.*) observations $\boldsymbol{x}_1, \ldots, \boldsymbol{x}_n$ from the nonparanormal model (1.1). Moreover, these variables follow a natural order such that banding/tapering estimation is meaningful.

We put the observed data in a $n \times p$ matrix $\boldsymbol{X}$. We can define $\boldsymbol{Z}_{ij} = f_j(\boldsymbol{X}_{ij})$, $1 \le i \le n; 1 \le j \le p$. We call $\boldsymbol{Z}$ the "oracle" data, because we would use them to estimate $\mathbf{\Sigma}$ if we knew the transformation functions. We begin with a key observation that $\sigma_{ij} = corr(f_i(X_i), f_j(X_j))$ for any (i, j) pair. We propose to use the rank correlation measure (Kendall (1948), Lehmann (1998)) to estimate entries of $\mathbf{\Sigma}$. Let $(x_{1i}, x_{2i}, \ldots, x_{ni})$ be the observed values of variable X_i and denote their ranks by $\boldsymbol{r}_i = (r_{1i}, r_{2i}, \ldots, r_{ni})$. We can estimate σ_{ij} by $\hat{r}^s_{ij}$ where

$$\hat{r}^s_{ij} = 2\sin(\frac{\pi}{6}\hat{r}_{ij}) \tag{2.1}$$

and

$$\hat{r}_{ij} = \frac{\sum_{l=1}^n (r_{li} - (n+1)/2)(r_{lj} - (n+1)/2)}{\sqrt{\sum_{l=1}^n (r_{li} - (n+1)/2)^2 \cdot \sum_{l=1}^n (r_{lj} - (n+1)/2)^2}}. \tag{2.2}$$

Note that $\hat{r}_{ij}$ is the Spearman's rank correlation and $\hat{r}^s_{ij}$ is called the adjusted Spearman's rank correlation (Kendall (1948)).

It is important to observe that $\boldsymbol{r}_i = (r_{1i}, r_{2i}, \ldots, r_{ni})$ are the ranks of the "oracle" data. The nonparanormal model implies that $f_i(X_i), f_j(X_j)$ follow a bivariate normal distribution with correlation parameter σ_{ij}, and a result due to Kendall (1948) is that

$$\lim_{n\to+\infty} \mathrm{E}(\hat{r}_{ij}) = \frac{6}{\pi}\arcsin(\frac{1}{2}\sigma_{ij}). \tag{2.3}$$

Thus the adjusted Spearman's rank correlation $\hat{r}^s_{ij}$ is an asymptotically unbiased estimator of σ_{ij}. Therefore adopt a rank-based sample estimate of $\boldsymbol{\Sigma}$,

$$\hat{\boldsymbol{R}}^s = (\hat{r}^s_{ij})_{1\le i,j\le p}. \tag{2.4}$$

When the dimension is large, $\hat{\boldsymbol{R}}^s$ performs poorly and we need to further consider a regularized version of the rank-based sample estimate. Banding or tapering is a useful regularization method when the variables have a natural order and off-diagonal entries of the target covariance matrix decay to zero as they move away from the diagonal. To provide a unified treatment of banding and tapering, we consider the generalized tapering estimator

$$\hat{\boldsymbol{R}}^s_{gt} = (\hat{r}^s_{ij} w_{ij})_{1\le i,j\le p},$$

where the generic tapering weights $(w_{ij})_{1\le i,j\le p}$ satisfy

(i) $w_{ij} = 1$ for $|i-j| \le k_h = \lfloor k/2 \rfloor$.

(ii) $w_{ij} = 0$ for $|i-j| > k$.

(iii) $0 \le w_{ij} \le 1$ for $k_h < |i-j| \le k$.

Banding weights (Bickel and Levina (2008a)) $w_{ij} = 1$ for $k_h < |i-j| \le k$, and tapering weights (Cai, Zhang, and Zhou (2010), Cai and Zhou (2012)) equal $w^{czz}_{ij} = (k - |i-j|)/k_h$ for $k_h < |i-j| \le k$. Both satisfy conditions (i)–(iii). The rank-based banding estimator is $\hat{\boldsymbol{R}}^s_b = (\hat{r}^s_{ij} I_{\{|i-j|\le k\}})_{1\le i,j\le p}$ and the rank-based tapering estimator is $\hat{\boldsymbol{R}}^s_t = (\hat{r}^s_{ij} w^{czz}_{ij})_{1\le i,j\le p}$. We consider the generalized tapering estimator because in some theoretical analyses the exact form of w_{ij} for $k_h < |i-j| \le k$ does not matter.

We would like to mention another "plug-in" tapering estimator of $\boldsymbol{\Sigma}$. One could first estimate the transformation functions to obtain the estimated "oracle" data as

$$\widehat{\boldsymbol{Z}}_{ij} = \hat{f}_j(\boldsymbol{X}_{ij}), \quad 1 \le i \le n; 1 \le j \le p,$$

where $\hat{f}_j$ is a good estimator of f_j. The final estimator is obtained by applying tapering to the sample covariance matrix of the estimated "oracle" data. Obviously, the "plug-in" tapering estimator requires more computations than the rank-based tapering estimator. This "plug-in" estimation idea was used by Liu, Lafferty, and Wasserman (2009) for estimating the inverse correlation matrix in the nonparanormal model. We discuss the theoretical advantages of the rank-based tapering estimator in Section 3.

The nonparanormal model is also interesting in the framework of graphical modeling. If $\boldsymbol{\Sigma}^{-1}$ is sparse in the sense that many entries of $\boldsymbol{\Sigma}^{-1}$ are exactly zero, then the few nonzero entries correspond to the edges in a nonparametric graphical model. Rank-based estimation techniques have been independently proposed in Xue and Zou (2012) and in Liu et al. (2012) for estimating sparse inverse correlation matrices of the nonparanormal model.

3. Theoretical Properties

We begin with some necessary notation and definitions. For a matrix $\boldsymbol{A} = (a_{ij})_{1\le i,j\le p}$, its Frobenius norm is $\|A\|_F = \sqrt{\sum_{i,j} a_{ij}^2}$, and its matrix ℓ_q-norm is the operator norm induced by the vector ℓ_q-norm,

$$\|\boldsymbol{A}\|_{\ell_v} = \sup_{\boldsymbol{u}} \frac{\|\boldsymbol{A}\boldsymbol{u}\|_{\ell_v}}{\|\boldsymbol{u}\|_{\ell_v}}.$$

The commonly used cases are $v = 1, 2, \infty$. The ℓ_1 norm is $\max_i \sum_j^p |a_{ij}|$ while the ℓ_∞ norm is $\max_j \sum_i^p |a_{ij}|$. For a symmetric matrix $\boldsymbol{A}$, $\|\boldsymbol{A}\|_{\ell_2}$ is the largest absolute value of its eigenvalues and $\|\boldsymbol{A}\|_{\ell_2} \le \|\boldsymbol{A}\|_{\ell_1} = \|\boldsymbol{A}\|_{\ell_\infty}$. For convenience, we use c and C to denote generic constants in lower and upper bounds, respectively.

For the theoretical analysis we assume that $\boldsymbol{\Sigma}$ is in a parameter space of bandable covariance matrices. Specifically, we consider the parameter spaces

$$\mathcal{H}_\alpha = \{\text{data follow model (1.1) and } \boldsymbol{\Sigma} \text{ satisfies } |\sigma_{ij}| \le \tau_1 |i-j|^{-(\alpha+1)} \text{ for } i \ne j\}.$$

$$\mathcal{F}_\alpha = \{\text{data follow model (1.1) and } \boldsymbol{\Sigma} \text{ satisfies} \max_j \sum_{i:|i-j|>k} |\sigma_{ij}| \le \tau_0 k^{-\alpha}, \text{ for all } k\},$$

In both spaces α specifies the rate of decay as σ_{ij} moves away from the diagonal. We assume $p \ge n$ and $\log p \le n^\kappa$ for some constant $\kappa \in (0,1)$. Note that $\log p/n \to 0$ is necessary for establishing consistency of any estimator of $\boldsymbol{\Sigma}$ (Cai, Zhang, and Zhou (2010), Cai and Zhou (2012)).

These parameter spaces are similar to those considered in previous work (Bickel and Levina (2008a), Cai, Zhang, and Zhou (2010), Cai and Zhou (2012)), but here we assume the data follow a nonparanormal distribution, while the previous papers assume sub-Gaussian data.

Theorem 1. *For the rank-based (generalized) tapering estimator* $\hat{\boldsymbol{R}}^s_{gt}$,

$$\sup_{\mathcal{H}_\alpha} \mathrm{E}\frac{1}{p}\big\|\hat{\boldsymbol{R}}^s_{gt} - \boldsymbol{\Sigma}\big\|_F^2 \le C\frac{k}{n} + Ck^{-2\alpha-1}.$$

With $k = n^{1/(2\alpha+2)}$, *the Frobenius risk bound is*

$$\sup_{\mathcal{H}_\alpha} \mathrm{E}\frac{1}{p}\big\|\hat{\boldsymbol{R}}^s_{gt} - \boldsymbol{\Sigma}\big\|_F^2 \le Cn^{-(2\alpha+1)/(2(\alpha+1))}. \tag{3.1}$$

Theorem 1 implies that the rank-based tapering estimator attains the minimax rate of convergence under the Frobenius norm. To see this, we cite a minimax lower bound from Cai, Zhang, and Zhou (2010) who constructed a special collection of multivariate distributions, denoted by $\mathcal{G}_2$, with $\inf_{\hat{\boldsymbol{\Sigma}}} \sup_{\mathcal{G}_2} \mathrm{E}\frac{1}{p}\big\|\hat{\boldsymbol{\Sigma}} - \boldsymbol{\Sigma}\big\|_F^2 \ge cn^{-(2\alpha+1)/(2\alpha+2)}$. See Section 4.2 of Cai, Zhang, and Zhou (2010) for details. Their $\mathcal{G}_2$ is a subspace of $\mathcal{H}_\alpha$ and hence

$$\inf_{\hat{\boldsymbol{\Sigma}}} \sup_{\mathcal{H}_\alpha} \mathrm{E}\frac{1}{p}\big\|\hat{\boldsymbol{\Sigma}} - \boldsymbol{\Sigma}\big\|_F^2 \ge \inf_{\hat{\boldsymbol{\Sigma}}} \sup_{\mathcal{G}_2} \mathrm{E}\frac{1}{p}\big\|\hat{\boldsymbol{\Sigma}} - \boldsymbol{\Sigma}\big\|_F^2 \ge cn^{-(2\alpha+1)/(2\alpha+2)}. \tag{3.2}$$

A comparison of (3.2) and (3.1) then establishes the minimax rate of convergence result.

Theorem 2. *For the rank-based (generalized) tapering estimator* $\hat{\boldsymbol{R}}^s_{gt}$,

$$\sup_{\mathcal{F}_\alpha} \mathrm{E}\big\|\hat{\boldsymbol{R}}^s_{gt} - \boldsymbol{\Sigma}\big\|_{\ell_a}^2 \le C\frac{k^2 \log p}{n} + Ck^{-2\alpha},$$

where $a = 1, 2$. *Moreover, if let* $k = (n/\log p)^{1/(2\alpha+2)}$, *then the* ℓ_a *risk bound* $(a = 1, 2)$ *is*

$$\sup_{\mathcal{F}_\alpha} \mathrm{E}\big\|\hat{\boldsymbol{R}}^s_{gt} - \boldsymbol{\Sigma}\big\|_{\ell_a}^2 \le C\left(\frac{\log p}{n}\right)^{\alpha/(\alpha+1)}. \tag{3.3}$$

Cai, Zhang, and Zhou (2010) and Cai and Zhou (2012) have established the lower bound results

$$\inf_{\hat{\boldsymbol{\Sigma}}} \sup_{\mathcal{G}^{**}} \mathrm{E}\big\|\hat{\boldsymbol{\Sigma}} - \boldsymbol{\Sigma}\big\|_{\ell_2}^2 \ge cn^{-2\alpha/(2\alpha+1)} + c\frac{\log(p)}{n}$$

$$\inf_{\hat{\boldsymbol{\Sigma}}} \sup_{\mathcal{G}^{*}} \mathrm{E}\big\|\hat{\boldsymbol{\Sigma}} - \boldsymbol{\Sigma}\big\|_{\ell_1}^2 \ge c\left(\frac{\log p}{n}\right)^{2\alpha/(2\alpha+1)} + cn^{-\alpha/(\alpha+1)}$$

where $\mathcal{G}^{**}$ and $\mathcal{G}^{*}$ are two carefully designed collections of multivariate normal distributions. We do not write down $\mathcal{G}^{**}$ and $\mathcal{G}^{*}$ here, see Section 3.2 of Cai, Zhang, and Zhou (2010) and Section 2.2 of Cai and Zhou (2012) for more details.

By definition, both $\mathcal{G}^{**}$ and $\mathcal{G}^{*}$ are subspaces of $\mathcal{F}_\alpha$. As a result, we have

$$\inf_{\hat{\boldsymbol{\Sigma}}} \sup_{\mathcal{F}_\alpha} \mathrm{E}\big\|\hat{\boldsymbol{\Sigma}} - \boldsymbol{\Sigma}\big\|_{\ell_2}^2 \ge cn^{-2\alpha/(2\alpha+1)} + c\frac{\log(p)}{n},$$

$$\inf_{\hat{\boldsymbol{\Sigma}}} \sup_{\mathcal{F}_\alpha} \mathrm{E}\big\|\hat{\boldsymbol{\Sigma}} - \boldsymbol{\Sigma}\big\|_{\ell_1}^2 \ge c\left(\frac{\log p}{n}\right)^{2\alpha/(2\alpha+1)} + cn^{-\alpha/(\alpha+1)}.$$

Theorem 2 does not then tell us whether the rank-based (generalized) tapering estimator is minimax rate optimal under the ℓ_1, ℓ_2 norms. Because we are dealing with the rank correlations, some key inequalities used in establishing upper bounds for the ℓ_1, ℓ_2 risk are no longer applicable, for example, the concentration bound for sub-Gaussian random variables (see page 2142 of Cai, Zhang, and Zhou (2010) and Saulis and Statulevičius (1991)). The proof of Theorem 2 uses a generalization of McDiarmid's inequality by Kutin (2002) and Kutin and Niyogi (2002).

With or without the minimax optimality, Theorems 1 and 2 show that the rank-based tapering estimator is uniformly consistent over a large parameter space, as long as the logarithm of the dimension grows slower than the sample size. Let us compare the rank-based tapering estimator and the "plug-in" tapering estimator. Liu, Lafferty, and Wasserman (2009) used a nonparametric density estimation scheme to estimate the transformation functions in the nonparanormal model and used the same "plug-in" idea to estimate $\mathbf{\Sigma}$ by applying the graphical lasso (Friedman, Hastie, and Tibshirani (2008)) to the estimated "oracle" data. Their theory is based on a concentration inequality that holds under the assumption that p is a polynomial order of n, but it is unclear whether the "plug-in" tapering estimator can still be consistent under nearly exponentially large dimensions.

4. Numerical Properties

In this section we report on both simulated data and real data to examine the finite-sample performance of the proposed rank-based tapering estimator.

4.1. Monte Carlo simulation

The main purpose of the simulation study was to show that the proposed rank-based tapering estimator works as well as the oracle tapering estimator. For the sake of completeness we also include the "plug-in" estimator for comparison.

We generated n independent p-dimension data points from the nonparanormal model (1.1) with $n = 200$ and $p = 200,\ 500$ and 1000. The $\mathbf{\Sigma}$ considered were as follows,

(1) $\sigma_{ij} = I_{\{i=j\}} + \rho|i-j|^{-(\alpha+1)} I_{\{i \neq j\}}$ with $\rho = 0.6$, and $\alpha = 0.1, 0.3, 0.5$.

(2) $\sigma_{ij} = \rho^{|i-j|}$ for $\rho = 0.3$ and 0.7.

(3) $\sigma_{ij} = I_{\{i=j\}} + \rho I_{\{|i-j|=1\}}$ for $\rho = 0.3$ and 0.5.

(4) $\sigma_{ij} = (1 - |i-j|/m)_+$ for $m = 0.1p$, $0.2p$ and $0.3p$.

The first was used in Cai, Zhang, and Zhou (2010); the second and third were used in Bickel and Levina (2008a,b) and Rothman, Levina, and Zhu (2009);

the fourth was studied in Cai and Liu (2011). We first generated n independent data from $N_p(0, \mathbf{\Sigma})$ and then transformed the normal data using transformation functions. In the simulation study we considered two sets of transformation functions for each $\mathbf{\Sigma}$: the identity transformation to obtain the normal data; the transformations $\boldsymbol{g} = [f_1^{-1}, f_2^{-1}, f_3^{-1}, f_4^{-1}, f_5^{-1}, f_1^{-1}, f_2^{-1}, f_3^{-1}, f_4^{-1}, f_5^{-1}, \ldots]$, where $f_1(x) = x$, $f_2(x) = \log(x)$, $f_3(x) = x^{1/3}$ and $f_4(x) = \log(\frac{x}{1-x})$.

The estimators considered in the study were the direct banding/tapering estimator, the proposed rank-based banding/tapering estimator and the "plug-in" estimator. See Table 1. To construct the "plug-in" estimator, we first estimated the "oracle" data $\hat{\boldsymbol{z}}_i = \widehat{\boldsymbol{f}}(\boldsymbol{x}_i)$ by applying the estimated transformation vector $\widehat{\boldsymbol{f}} = (\hat{f}_1, \cdots, \hat{f}_p) = (\Phi^{-1} \circ \hat{F}_1, \cdots, \Phi^{-1} \circ \hat{F}_p)$ with $\hat{F}_j$ a Winsorized estimator of the CDF of X_j (Liu, Lafferty, and Wasserman (2009)), and then performed the banding/tapering procedure over the estimated "oracle" data. By our simulation design, no matter which transformation function was used to generate the nonparanormal data, the "oracle" data were always the normal data on which the transformation is applied. Therefore, although the direct banding/tapering estimator is obviously wrong for the nonparanormal data, their results on the normal data are actually the results of the ideal banding/tapering estimator for both normal and nonparanormal data cases, which can be used as the benchmark for comparison. We only report the results of direct banding/tapering for the normal data. Each estimator was tuned by 5-fold cross-validation. The estimation accuracy was measured by the average ℓ_1-norm over 100 independent replications.

The simulation results are summarized in Tables 2−5. We can draw several conclusions. First, the rank-based banding/tapering estimators work very similarly to the ideal banding/tapering estimator, whose results correspond to those by the direct banding/tapering estimator on normal data. The rank-based estimator is only slightly worse than the ideal estimator, which is expected because some information is lost in the process of converting the original data into their ranks. The rank-based estimators outperform the "plug-in" estimators. We also compared these estimators using Frobenius norm and ℓ_2 norm. The conclusions stay the same. For the sake of space we do not present the simulation results under Frobenius norm and ℓ_2 norm here.

4.2. Applications to the rock spectrum data

We use the rock sonar spectrum data (Gorman and Sejnowski (1988)) to illustrate the nonparanormal model and the efficacy of the proposed rank-based banding/tapering estimator. This dataset consists of 97 sonar spectra bounced off roughly cylindrical rocks under similar conditions, and each spectrum has 60 frequency-band energy measurements in the range 0.0 to 1.0. We first conducted

Table 1. List of estimators in the simulation study.

Notation	Meaning
$\hat{\boldsymbol{\Sigma}}_b^d$	the direct banding estimator
$\hat{\boldsymbol{\Sigma}}_t^d$	the direct tapering estimator
$\hat{\boldsymbol{R}}_b^s$	the rank-based banding estimator
$\hat{\boldsymbol{R}}_t^s$	the rank-based tapering estimator
$\hat{\boldsymbol{\Sigma}}_b^p$	the "plug-in" banding estimator
$\hat{\boldsymbol{\Sigma}}_t^p$	the "plug-in" tapering estimator

Table 2. Simulation results under (1). Estimation accuracy is measured by the ℓ_1-norm averaged over 100 replications. The standard errors are shown in the bracket. In this study, the direct banding/tapering estimator on the normal data corresponds to an ideal banding/tapering estimator on both normal and nonparanormal data.

α	0.1			0.3			0.5		
p	200	500	1000	200	500	1000	200	500	1000
				normal data					
$\hat{\boldsymbol{\Sigma}}_b^d$	3.50	4.27	4.78	2.35	2.67	2.86	1.68	1.83	1.92
	(0.01)	(0.02)	(0.02)	(0.01)	(0.01)	(0.02)	(0.01)	(0.01)	(0.01)
$\hat{\boldsymbol{R}}_b^s$	3.55	4.33	4.82	2.39	2.71	2.90	1.71	1.86	1.95
	(0.01)	(0.02)	(0.02)	(0.01)	(0.01)	(0.02)	(0.01)	(0.01)	(0.01)
$\hat{\boldsymbol{\Sigma}}_b^p$	3.57	4.34	4.88	2.43	2.75	2.95	1.76	1.92	2.01
	(0.01)	(0.02)	(0.02)	(0.01)	(0.02)	(0.02)	(0.01)	(0.01)	(0.02)
$\hat{\boldsymbol{\Sigma}}_t^d$	3.40	4.19	4.71	2.28	2.60	2.80	1.64	1.81	1.92
	(0.01)	(0.02)	(0.02)	(0.01)	(0.02)	(0.02)	(0.01)	(0.01)	(0.02)
$\hat{\boldsymbol{R}}_t^s$	3.46	4.25	4.76	2.32	2.65	2.85	1.68	1.84	1.94
	(0.01)	(0.02)	(0.02)	(0.01)	(0.02)	(0.02)	(0.01)	(0.01)	(0.02)
$\hat{\boldsymbol{\Sigma}}_t^p$	3.52	4.30	4.84	2.39	2.72	2.93	1.75	1.91	2.02
	(0.02)	(0.02)	(0.02)	(0.01)	(0.02)	(0.02)	(0.01)	(0.01)	(0.02)
				nonparanormal data					
$\hat{\boldsymbol{R}}_b^s$	3.55	4.33	4.82	2.39	2.71	2.90	1.71	1.86	1.95
	(0.01)	(0.02)	(0.02)	(0.01)	(0.01)	(0.02)	(0.01)	(0.01)	(0.01)
$\hat{\boldsymbol{\Sigma}}_b^p$	3.57	4.34	4.88	2.43	2.75	2.95	1.76	1.92	2.01
	(0.01)	(0.02)	(0.02)	(0.01)	(0.02)	(0.02)	(0.01)	(0.01)	(0.02)
$\hat{\boldsymbol{R}}_t^s$	3.46	4.25	4.76	2.32	2.65	2.85	1.68	1.84	1.94
	(0.01)	(0.02)	(0.02)	(0.01)	(0.02)	(0.02)	(0.01)	(0.01)	(0.02)
$\hat{\boldsymbol{\Sigma}}_t^p$	3.52	4.30	4.84	2.39	2.72	2.93	1.75	1.91	2.02
	(0.02)	(0.02)	(0.02)	(0.01)	(0.02)	(0.02)	(0.01)	(0.01)	(0.02)

normality tests on the 60 spectra signals to check for serious violations of normality. The test results are reported in Table 6. More than 80% of the signals are unable to pass any of four normality tests, and under Bonferroni correction there are still over 50% that fail to pass the tests. As this is a strong indication

Table 3. Simulation results under (2). Estimation accuracy is measured by the ℓ_1-norm averaged over 100 replications. The standard errors are shown in the bracket. In this study, the direct banding/tapering estimator on the normal data corresponds to an ideal banding/tapering estimator on both normal and nonparanormal data.

ρ	0.3			0.7		
p	200	500	1000	200	500	1000
			normal data			
$\hat{\boldsymbol{\Sigma}}_b^d$	0.57 (0.01)	0.61 (0.01)	0.64 (0.01)	1.74 (0.01)	1.85 (0.02)	1.94 (0.02)
$\hat{\boldsymbol{R}}_b^s$	0.59 (0.01)	0.63 (0.01)	0.67 (0.01)	1.80 (0.02)	1.91 (0.02)	2.00 (0.03)
$\hat{\boldsymbol{\Sigma}}_b^p$	0.62 (0.01)	0.66 (0.01)	0.69 (0.01)	1.89 (0.02)	2.02 (0.02)	2.11 (0.03)
$\hat{\boldsymbol{\Sigma}}_t^d$	0.59 (0.01)	0.62 (0.01)	0.66 (0.01)	1.67 (0.02)	1.80 (0.02)	1.90 (0.03)
$\hat{\boldsymbol{R}}_t^s$	0.60 (0.01)	0.62 (0.01)	0.63 (0.01)	1.74 (0.02)	1.87 (0.02)	1.96 (0.03)
$\hat{\boldsymbol{\Sigma}}_t^p$	0.63 (0.01)	0.67 (0.01)	0.70 (0.01)	1.87 (0.02)	2.01 (0.02)	2.10 (0.03)
			nonparanormal data			
$\hat{\boldsymbol{R}}_b^s$	0.59 (0.01)	0.63 (0.01)	0.67 (0.01)	1.80 (0.02)	1.91 (0.02)	2.00 (0.03)
$\hat{\boldsymbol{\Sigma}}_b^p$	0.62 (0.01)	0.66 (0.01)	0.69 (0.01)	1.89 (0.02)	2.02 (0.02)	2.11 (0.03)
$\hat{\boldsymbol{R}}_t^s$	0.60 (0.01)	0.62 (0.01)	0.63 (0.01)	1.74 (0.02)	1.87 (0.02)	1.96 (0.03)
$\hat{\boldsymbol{\Sigma}}_t^p$	0.63 (0.01)	0.67 (0.01)	0.70 (0.01)	1.87 (0.02)	2.01 (0.02)	2.10 (0.03)

that the normal assumption does not hold here, we considered the more robust nonparanormal model for this dataset.

For each spectrum, the 60 signals were obtained from an increasing order of 60 aspect angles spanning 180 degrees, so there is a natural order among signals for each spectra. The physical nature of the data motivates us to estimate its bandable correlation matrix structure. Moreover, the heatmap of the Spearman's correlation matrix given in Figure 1 shows a general decaying pattern that suggests that it is quite reasonable to assume the correlation matrix of the nonparanormal model is bandable. Thus we computed the rank-based banding/tapering estimators. The rank-based banding estimator selected $\hat{k} = 27$ sub-diagonals by cross-validation, while the rank-based tapering estimator selected $\hat{k} = 38$ sub-diagonals. The heatmaps of the absolute values of the rank-based banding/tapering estimators are shown in Figure 2.

Table 4. Simulation results under (3). Estimation accuracy is measured by the ℓ_1-norm averaged over 100 replications. The standard errors are shown in the bracket. In this study, the direct banding/tapering estimator on the normal data corresponds to an ideal banding/tapering estimator on both normal and nonparanormal data.

ρ	0.3			0.5		
p	200	500	1000	200	500	1000
	normal data					
$\hat{\boldsymbol{\Sigma}}_b^d$	0.29 (0.00)	0.31 (0.01)	0.34 (0.01)	0.24 (0.00)	0.27 (0.00)	0.28 (0.01)
$\hat{\boldsymbol{R}}_b^s$	0.31 (0.00)	0.33 (0.00)	0.35 (0.01)	0.26 (0.00)	0.29 (0.00)	0.30 (0.01)
$\hat{\boldsymbol{\Sigma}}_b^p$	0.35 (0.00)	0.37 (0.01)	0.39 (0.01)	0.32 (0.00)	0.34 (0.00)	0.35 (0.01)
$\hat{\boldsymbol{\Sigma}}_t^d$	0.29 (0.00)	0.31 (0.01)	0.34 (0.01)	0.24 (0.00)	0.27 (0.00)	0.28 (0.01)
$\hat{\boldsymbol{R}}_t^s$	0.31 (0.00)	0.33 (0.00)	0.35 (0.01)	0.26 (0.00)	0.29 (0.00)	0.30 (0.01)
$\hat{\boldsymbol{\Sigma}}_t^p$	0.35 (0.00)	0.37 (0.01)	0.39 (0.01)	0.32 (0.00)	0.34 (0.00)	0.35 (0.01)
	nonparanormal data					
$\hat{\boldsymbol{R}}_b^s$	0.31 (0.00)	0.33 (0.00)	0.35 (0.01)	0.26 (0.00)	0.29 (0.00)	0.30 (0.01)
$\hat{\boldsymbol{\Sigma}}_b^p$	0.35 (0.00)	0.37 (0.01)	0.39 (0.01)	0.32 (0.00)	0.34 (0.00)	0.35 (0.01)
$\hat{\boldsymbol{R}}_t^s$	0.31 (0.00)	0.33 (0.00)	0.35 (0.01)	0.26 (0.00)	0.29 (0.00)	0.30 (0.01)
$\hat{\boldsymbol{\Sigma}}_t^p$	0.35 (0.00)	0.37 (0.01)	0.39 (0.01)	0.32 (0.00)	0.34 (0.00)	0.35 (0.01)

Under the nonparanormal model, if the correlation matrix is exactly banded then the direct correlation matrix of the raw data is as well. Accordingly, we expect that if a nonparanormal model with an exactly banded correlation matrix is a good fit to the rock spectrum data, then a similar bandable structure also holds for the direct correlation matrix of the raw data. We performed the direct banding/tapering procedures on the raw data and we did obtain the same bandable structure: the direct banding chose $\hat{k} = 27$ sub-diagonals and the direct tapering selected $\hat{k} = 38$ sub-diagonals. We show the heatmaps of the absolute values of the direct banding/tapering estimators in Figure 3, providing more support to the fitted nonparanormal model.

5. Discussion

We have introduced a rank-based generalized tapering estimator for esti-

Table 5. Simulation results under (4). Estimation accuracy is measured by the ℓ_1-norm averaged over 100 replications. The standard errors are shown in the bracket. In this study, the direct banding/tapering estimator on the normal data corresponds to an ideal banding/tapering estimator on both normal and nonparanormal data.

m	0.1p			0.2p			0.3p		
p	200	500	1000	200	500	1000	200	500	1000
				normal data					
$\hat{\mathbf{\Sigma}}_b^d$	1.55	3.99	8.06	2.87	7.52	15.58	5.20	13.70	28.33
	(0.02)	(0.08)	(0.19)	(0.05)	(0.15)	(0.56)	(0.11)	(0.41)	(1.14)
$\hat{\boldsymbol{R}}_b^s$	1.67	4.22	8.82	3.08	8.13	16.64	5.55	14.57	30.59
	(0.03)	(0.09)	(0.21)	(0.05)	(0.17)	(0.55)	(0.10)	(0.41)	(1.26)
$\hat{\mathbf{\Sigma}}_b^p$	1.88	4.77	9.86	3.48	9.26	18.47	6.47	16.44	33.92
	(0.03)	(0.08)	(0.22)	(0.06)	(0.29)	(0.57)	(0.11)	(0.44)	(1.23)
$\hat{\mathbf{\Sigma}}_t^d$	1.63	4.19	8.56	3.07	8.02	16.50	5.25	13.70	27.97
	(0.03)	(0.09)	(0.22)	(0.06)	(0.21)	(0.61)	(0.09)	(0.35)	(1.11)
$\hat{\boldsymbol{R}}_t^s$	1.73	4.40	9.25	3.20	8.48	17.41	5.64	14.62	30.65
	(0.03)	(0.10)	(0.22)	(0.05)	(0.20)	(0.64)	(0.10)	(0.37)	(1.29)
$\hat{\mathbf{\Sigma}}_t^p$	2.06	5.21	10.79	3.80	10.12	20.20	6.85	17.47	36.09
	(0.03)	(0.09)	(0.24)	(0.06)	(0.27)	(0.63)	(0.13)	(0.41)	(1.36)
				nonparanormal data					
$\hat{\boldsymbol{R}}_b^s$	1.67	4.22	8.82	3.08	8.13	16.64	5.55	14.57	30.59
	(0.03)	(0.09)	(0.21)	(0.05)	(0.17)	(0.55)	(0.10)	(0.41)	(1.26)
$\hat{\mathbf{\Sigma}}_b^p$	1.88	4.77	9.86	3.48	9.26	18.47	6.47	16.44	33.92
	(0.03)	(0.08)	(0.22)	(0.06)	(0.29)	(0.57)	(0.11)	(0.44)	(1.23)
$\hat{\boldsymbol{R}}_t^s$	1.73	4.40	9.25	3.20	8.48	17.41	5.64	14.62	30.65
	(0.03)	(0.10)	(0.22)	(0.05)	(0.20)	(0.64)	(0.10)	(0.37)	(1.29)
$\hat{\mathbf{\Sigma}}_t^p$	2.06	5.21	10.79	3.80	10.12	20.20	6.85	17.47	36.09
	(0.03)	(0.09)	(0.24)	(0.06)	(0.27)	(0.63)	(0.13)	(0.41)	(1.36)

Table 6. Normality test results for the rock spectrum data. The counts of spectra that fail to pass each normality test are shown in the table.

critical value	Anderson–Darling	Cramér–von Mises	Lilliefors	Shapiro-Francia
0.05	55	52	48	56
0.05/60	45	41	31	43

mating a high-dimensional correlation matrix in the nonparanormal model. The theoretical and numerical examples have provided strong support for this estimation method. Tapering estimation requires a natural order among the variables, if there is no such order information, it is better to use a permutation invariance estimator such as thresholding. In Xue and Zou (2011) we have shown the adaptive minimax optimality of a rank-based thresholding estimator for estimating sparse correlation matrices of nonparanormal models.

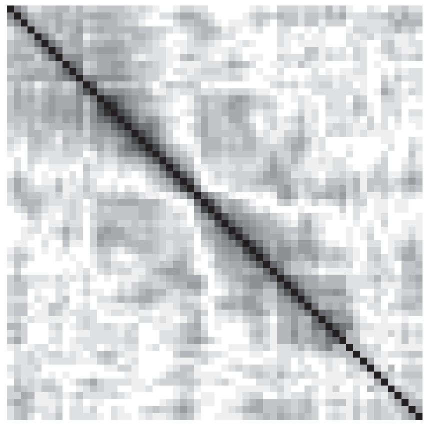

Figure 1. Heapmap of the absolute values of Spearman's correlation matrix for the rock spectrum data. White means zero correlation and black means perfect correlation (magnitude equals 1).

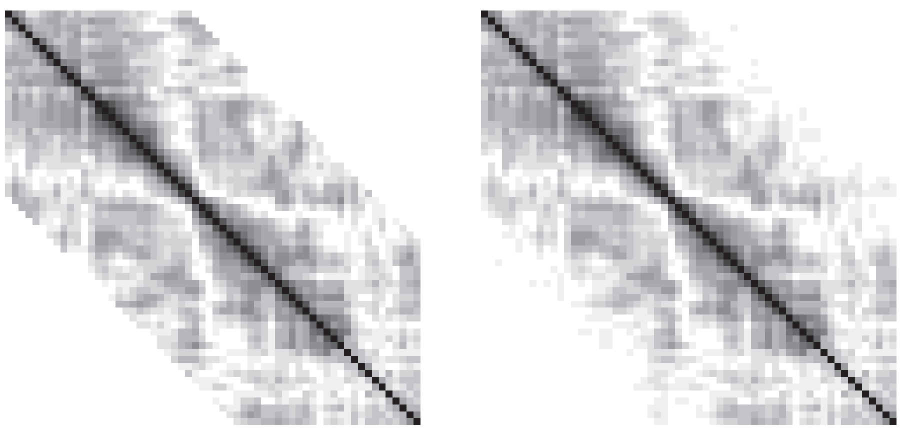

(A): rank-based banding estimation. (B): rank-based tapering estimation.

Figure 2. Heapmaps of the absolute values of the rank-based banding/tapering estimator for the rock spectrum data.

Appendix: Technical proofs

We first present a useful lemma on concentration bounds toward the accuracy of the rank-based sample estimator. The proof is in Xue and Zou (2012).

Lemma A.1. *Fix any* $0 < \varepsilon < 1$ *and let* $n \geq 12\pi/\varepsilon$. *We have*

$$\Pr(|\hat{r}_{ij}^s - \sigma_{ij}| > \varepsilon) \leq 2\exp(-c_0 n\varepsilon^2),$$
$$\Pr(\|\hat{\boldsymbol{R}}^s - \boldsymbol{\Sigma}\|_{\max} > \varepsilon) \leq p^2 \exp(-c_0 n\varepsilon^2),$$

where $\|\hat{\boldsymbol{R}}^s - \boldsymbol{\Sigma}\|_{\max} = \max_{(i,j)} |\hat{r}_{ij}^s - \sigma_{ij}|$ *is the max norm, and* c_0 *is some absolute*

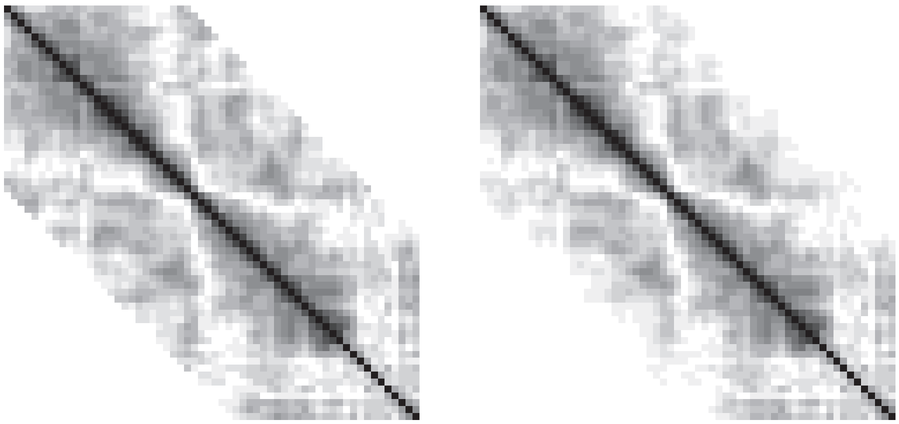

(A): direct banding estimation on the raw data. (B): direct tapering estimation on the raw data.

Figure 3. Heapmaps of the absolute values of the direct banding/tapering estimator for the rock spectrum data.

constant.

Proof of Theorem 1. With $\mathbf{\Gamma}_b = (\sigma_{ij} I_{\{|i-j|\leq k\}})_{1\leq i,j\leq p}$ and $\mathbf{\Gamma}_{gt} = (\sigma_{ij} w_{ij})_{1\leq i,j\leq p}$ and we have

$$\mathrm{E}\big\|\hat{\boldsymbol{R}}^s_{gt} - \mathbf{\Sigma}\big\|_F^2 \leq \mathrm{E}\big\|\hat{\boldsymbol{R}}^s_{gt} - \mathbf{\Gamma}_{gt}\big\|_F^2 + \big\|\mathbf{\Gamma}_{gt} - \mathbf{\Gamma}_b\big\|_F^2 + \big\|\mathbf{\Gamma}_b - \mathbf{\Sigma}\big\|_F^2.$$

By the assumption $|\sigma_{ij}| \leq \tau_1 |i-j|^{-(\alpha+1)}$ for $i \neq j$ and $0 \leq w_{ij} \leq 1$, one has $\big\|\mathbf{\Gamma}_{gt} - \mathbf{\Gamma}_b\big\|_F^2 \leq Cpk^{-2\alpha-2}$. We can also derive the upper bound for $\big\|\mathbf{\Gamma}_b - \mathbf{\Sigma}\big\|_F^2$ as

$$\big\|\mathbf{\Gamma}_b - \mathbf{\Sigma}\big\|_F^2 \leq 2\tau_1 \cdot \sum_{m=k+1}^{p-1} m^{-2(\alpha+1)} \leq 2\tau_1 \cdot pk^{-2\alpha-1}, \tag{A.1}$$

where we use the fact that

$$\sum_{m=k+1}^{p-1} m^{-2(\alpha+1)} \leq \int_k^{+\infty} t^{-2(\alpha+1)} dt \leq \frac{1}{2\alpha} k^{-2\alpha-1}.$$

On the other hand, $(\hat{r}^s_{ij} - \sigma_{ij})^2 \leq (2\pi^2/9)(u_{ij} - E(u_{ij}))^2 + O(1/n^2)$ holds by the Hoeffding decomposition of $\hat{r}_{ij}$. Note that $\mathrm{Var}(u_{ij}) = O(1/n)$, and then it can be seen that

$$\mathrm{E}\frac{1}{p}\big\|\hat{\boldsymbol{R}}^s_{gt} - \mathbf{\Gamma}_{gt}\big\|_F^2 \leq \mathrm{E}\frac{1}{p}\big\|\hat{\boldsymbol{R}}^s_{b} - \mathbf{\Gamma}_{b}\big\|_F^2 \leq \frac{2\pi^2}{9} k \cdot (\max_{i,j} \mathrm{Var}(u_{ij}) + \frac{c}{n^2}) \leq C\frac{k}{n}. \tag{A.2}$$

Combining (A.1) and (A.2) concludes the proof by noting that

$$\mathrm{E}\frac{1}{p}\big\|\hat{\boldsymbol{R}}^s_{gt} - \mathbf{\Sigma}\big\|_F^2 \leq C\frac{k}{n} + Ck^{-2\alpha-1}.$$

Proof of Theorem 2. We only need to prove the ℓ_1 risk bound, the ℓ_2 risk bound follows from the fact that the ℓ_2 norm is upper bounded by the ℓ_1 norm. Introduce the ideal generalized tapering estimator $\mathbf{\Gamma}_{gt} = (\sigma_{ij} w_{ij})_{1\le i,j\le p}$. The sub-additive property of the matrix ℓ_1-norm implies that

$$\mathrm{E}\big\|\hat{\boldsymbol{R}}^s_{gt} - \mathbf{\Sigma}\big\|^2_{\ell_1} \le 2\mathrm{E}\big\|\hat{\boldsymbol{R}}^s_{gt} - \mathbf{\Gamma}_{gt}\big\|^2_{\ell_1} + 2\big\|\mathbf{\Gamma}_{gt} - \mathbf{\Sigma}\big\|^2_{\ell_1}. \tag{A.3}$$

Note that $0 \le w_{ij} \le 1$ for any (i, j) and $w_{ij} = 1$ when $|i - j| \le k_h$, and so

$$\big\|\mathbf{\Gamma}_{gt} - \mathbf{\Sigma}\big\|^2_{\ell_1} \le \big(\max_{i=1,\ldots,p} \sum_{i:\ |i-j|>k_h} |\sigma_{ij}|\big)^2 \le \tau_0^2 k_h^{-2\alpha}.$$

Now, we only need to bound $\mathrm{E}\big\|\hat{\boldsymbol{R}}^s_{gt} - \mathbf{\Gamma}_{gt}\big\|^2_{\ell_1}$. Since $0 \le w_{ij} \le 1$ for any (i, j) and $w_{ij} = 0$ for $|i - j| > k$, we can derive an upper bound as follows,

$$\begin{aligned}\big\|\hat{\boldsymbol{R}}^s_{gt} - \mathbf{\Gamma}_{gt}\big\|^2_{\ell_1} &\le \max_{1\le i\le p}\Big(\sum_{i-k\le j\le i+k} |\hat{r}^s_{ij} - \sigma_{ij}|\Big)^2 \\ &\le (2k+1)\cdot \max_{1\le i\le p} \sum_{i-k\le j\le i+k} (\hat{r}^s_{ij} - \sigma_{ij})^2.\end{aligned}$$

Recall that $\hat{r}^s_{ij} = 2\sin((\pi/6)\hat{r}_{ij})$ and $\sigma_{ij} = 2\sin((\pi/6)E(u_{ij}))$. To further simplify the upper bound, we consider the Hoeffding decomposition of $\hat{r}_{ij}$ (Hoeffding (1948)),

$$\begin{aligned}(\hat{r}^s_{ij} - \sigma_{ij})^2 &\le \frac{\pi^2}{9}(\hat{r}_{ij} - E(u_{ij}))^2 \\ &\le \frac{2\pi^2}{9}\big[(u_{ij} - E(u_{ij}))^2 + (\frac{3}{n+1}u_{ij} - \frac{3}{n^3-n}d_{ij})^2\big] \\ &= \frac{2\pi^2}{9}(u_{ij} - E(u_{ij}))^2 + O(\frac{1}{n^2}),\end{aligned}$$

where $d_{ij} = \sum_{i_1\ne i_2} \mathrm{sign}(x_{i_1 i} - x_{i_2 i}) \cdot \mathrm{sign}(x_{i_1 j} - x_{i_2 j})$.

Now we derive the concentration bound for

$$U_i^{(k)} = \sum_{i-k\le j\le i+k} (u_{ij} - E(u_{ij}))^2.$$

We consider the generalization of McDiarmid's inequality by Kutin (2002) and Kutin and Niyogi (2002) when differences are bounded with high probability. Note that $U_i^{(k)}$ can be considered as a function of independent samples $\boldsymbol{x}_1, \ldots, \boldsymbol{x}_n$, $U_i^{(k)} = U_i^{(k)}(\boldsymbol{x}_1, \ldots, \boldsymbol{x}_n)$. We replace the t-th sample $\boldsymbol{x}_t$ by another independent sample $\tilde{\boldsymbol{x}}_t$, and take

$$\tilde{U}_i^{(k)} = U_i^{(k)}(\boldsymbol{x}_1, \ldots, \boldsymbol{x}_{t-1}, \tilde{\boldsymbol{x}}_t, \boldsymbol{x}_{t+1}, \ldots, \boldsymbol{x}_n)$$

and $\tilde{u}_{ij} = u_{ij}(\boldsymbol{x}_1, \ldots, \boldsymbol{x}_{t-1}, \tilde{\boldsymbol{x}}_t, \boldsymbol{x}_{t+1}, \ldots, \boldsymbol{x}_n)$. We have that

$$|U_i^{(k)} - \tilde{U}_i^{(k)}| \le \sum_{i-k \le j \le i+k} |(u_{ij} - E(u_{ij}))^2 - (\tilde{u}_{ij} - E(\tilde{u}_{ij}))^2|$$
$$\le 12 \sum_{i-k \le j \le i+k} |u_{ij} - \tilde{u}_{ij}| \le c_1 \frac{k}{n},$$

where c_1 is some absolute constant. We use the facts that $|u_{ij}| \le 3$ and $|\tilde{u}_{ij}| \le 3$ in the first inequality, and $|u_{ij} - \tilde{u}_{ij}| \le 15/n$ (Xue and Zou (2012)) in the last inequality. Moreover, under the probability event that

$$\{\max_{i,j} |u_{ij} - E(u_{ij})| \le \epsilon\} \cap \{\max_{i,j} |\tilde{u}_{ij} - E(\tilde{u}_{ij})| \le \epsilon\} \text{ with } \epsilon^2 = c_0 M \frac{\log p}{n}$$

for $M > 0$, $U_i^{(k)} - \tilde{U}_i^{(k)}$ can be upper bounded as

$$|U_i^{(k)} - \tilde{U}_i^{(k)}| \le \sum_{i-k \le j \le i+k} (|u_{ij} - E(u_{ij})| + |\tilde{u}_{ij} - E(u_{ij})|) \cdot |u_{ij} - \tilde{u}_{ij}| \le c_2 M \frac{k \log^{1/2} p}{n^{3/2}},$$

where c_2 is some absolute constant. Thus,

$$\Pr(|U_i^{(k)} - \tilde{U}_i^{(k)}| > c_2 M \frac{k \log p}{n^{3/2}}) \le 2 \Pr(\max_{ij} |u_{ij} - E(u_{ij})| > \epsilon) \le 4p^{-M}.$$

Using the terminology from Kutin (2002) and Kutin and Niyogi (2002), we have proved that $U_i^{(k)}$ is strongly difference-bounded by

$$(b_*, c_*, \delta_*) \equiv \Big(c_1 \frac{k}{n}, c_2 M \frac{k \log^{1/2} p}{n^{3/2}}, 4p^{-M}\Big).$$

We directly apply Theorem 2.13 in Kutin and Niyogi (2002), which is a simplified version of Theorem 1.9 in Kutin (2002), to obtain

$$\Pr(U_i^{(k)} - E(U_i^{(k)}) > \frac{x^2}{n}) \le \exp(\frac{-x^4/n^2}{8nc_*^2}) + \frac{nb_*\delta_*}{c_*}$$
$$= \exp(\frac{-x^4}{8c_2^2 M^2 k^2 \log p}) + \frac{4c_1}{c_2 M} \cdot n^{3/2} p^{-M} \log^{-1/2} p.$$

Since (5.13) in Hoeffding (1948) showed that $\mathrm{Var}(u_{ij}) = O(1/n)$ for any (i, j), we have $E[U_i^{(k)}] = O(k/n)$. Now applying the union bound yields that, for some constant $C_0 > 0$,

$$\Pr\big(\max_{1 \le i \le p} U_i^{(k)} > C_0(\frac{k}{n} + \frac{x^2}{n})\big) \le p \cdot \max_{1 \le i \le p} \Pr(U_i^{(k)} - E(U_i^{(k)}) > \frac{x^2}{n}).$$

We are ready to bound the expected ℓ_1-norm of $\hat{\boldsymbol{R}}^s_{gt} - \boldsymbol{\Gamma}_{gt}$ by truncation of $\max\limits_{1\le i\le p} U_i^{(k)}$:

$$
\begin{aligned}
\mathrm{E}\big\|\hat{\boldsymbol{R}}^s_{gt} - \boldsymbol{\Gamma}_{gt}\big\|^2_{\ell_1} &\le C\frac{k^2}{n^2} + \frac{2\pi^2}{9}(2k+1)\mathrm{E}(\max_{1\le i\le p} U_i^{(k)}) \\
&\le C\frac{k^2}{n^2} + Ck\cdot \mathrm{E}[\max_{1\le i\le p} U_i^{(k)}(I_{\{\max\limits_{1\le i\le p} U_i^{(k)} \le C_0(\frac{k}{n}+\frac{x^2}{n})\}} \\
&\quad + I_{\{\max\limits_{1\le i\le p} U_i^{(k)} > C_0(\frac{k}{n}+\frac{x^2}{n})\}})] \\
&\le C\frac{k^2}{n^2} + C(\frac{k^2}{n} + \frac{kx^2}{n}) + Ck^2\cdot \Pr\Big(\max_{1\le i\le p} U_i^{(k)} > C(\frac{k}{n}+\frac{x^2}{n})\Big) \\
&\le C_1(\frac{k^2}{n} + \frac{kx^2}{n}) + C_2k^2p\exp(-\frac{x^4}{8c_2^2M^2k^2\log p}) \\
&\quad + C_3k^2n^{3/2}p^{-M+1}(\log p)^{-1/2},
\end{aligned}
$$

where we use the fact that $|U_i^{(k)}| = O(k)$ in the last but one inequality. Thus we choose $M > 4$, and further set $x^4 = 8c_2^2M^3\cdot k^2\log^2 p$ to conclude that

$$
\mathrm{E}\big\|\hat{\boldsymbol{R}}^s_{gt} - \boldsymbol{\Sigma}\big\|^2_{\ell_1} \le C\frac{k^2\log p}{n} + Ck^{-2\alpha}.
$$

References

Bickel, P. and Levina, E. (2008a). Regularized estimation of large covariance matrices. *Ann. Statist.* **36**, 199-227.

Bickel, P. and Levina, E. (2008b). Covariance regularization by thresholding. *Ann. Statist.* **36**, 2577-2604.

Cai, T. and Liu, W. (2011). Adaptive thresholding for sparse covariance matrix estimation, *J. Amer. Statist. Assoc.* **106**, 672-684.

Cai, T., Zhang, C. and Zhou, H. (2010). Optimal rates of convergence for covariance matrix estimation. *Ann. Statist.* **38**, 2118-2144.

Cai, T. and Zhou, H. (2012). Minimax estimation of large covariance matrices under ℓ_1-norm (with discussion). *Statist. Sinica* **22**, 1319-1378.

Chen, X. and Fan, Y. (2006). Estimation of copula-based semiparametric time series models, *J. Econom.* **130**, 307-335.

Chen, X., Fan, Y. and Tsyrennikov, V. (2006). Efficient estimation of semiparametric multivariate copula models, *J. Amer. Statist. Assoc.* **101**, 1228-1240.

El Karoui, N. (2008). Operator norm consistent estimation of large dimensional sparse covariance matrices, *Ann. Statist.* **36**, 2717-2756.

Friedman, J., Hastie, T. and Tibshirani, R. (2008). Sparse inverse covariance estimation with the graphical lasso. *Biostatistics* **9**, 432-441.

Furrer, R. and Bengtsson, T. (2007). Estimation of high-dimensional prior and posterior covariance matrices in Kalman filter variants. *J. Multivariate Anal.* **98**, 227-255.

Gorman, R. and Sejnowski, T. (1988). Analysis of hidden units in a layered network trained to classify sonar targets. *Neural Networks* **1**, 75-89.

Hoeffding, W. (1948). A class of statistics with asymptotically normal distribution. *Ann. Math. Statist.* **19**, 293-325.

Johnstone, I. (2001). On the distribution of the largest eigenvalue in principal components analysis. *Ann. Statist.* **29**, 295-327.

Kendall, M. (1948). *Rank Correlation Methods*. Charles Griffin, London.

Klaassen, C. and Wellner, J. (1997). Efficient estimation in the bivariate normal copula model: normal margins are least favourable. *Bernoulli* **3**, 55-77.

Kutin, S. (2002). Extensions to McDiarmid's inequality when differences are bounded with high probability. Technical report. TR-2002-04, University of Chicago.

Kutin, S. and Niyogi, P. (2002). Almost-everywhere algorithmic stability and generalization error, *Proceedings of the eighteenth conference on Unvertainty in Artifical Intelligence*, 275-282

Lehmann, E. (1998). *Nonparametrics: Statistical Methods Based on Ranks*. Prentice Hall Upper Saddle River, New Jersey.

Liu, H., Han, F., Yuan, M., Lafferty, J. and Wasserman, L. (2012). High dimensional semiparametric Gaussian copula graphical models. *Ann. Statist.*, in press.

Liu, H., Lafferty, J. and Wasserman, L. (2009). The nonparanormal: semiparametric estimation of high dimensional undirected graphs. *J. Mach. Learn. Res.* **10**, 1-37.

Rothman, A., Levina, E. and Zhu, J. (2009). Generalized thresholding of large covariance matrices. *J. Amer. Statist. Assoc.* **104**, 177-186.

Rothman, A., Levina, E. and Zhu, J. (2010). A new approach to Cholesky-based covariance regularization in high dimensions. *Biometrika* **97**, 539-550.

Saulis, L. and Statulevičius, V. (1991). *Limit Theorems for Large Deviations*. Springer, Berlin.

Song, P. (2000). Multivariate dispersion models generated from gaussian copula. *Scand. J. Statist.* **27**, 305-320.

Song, P., Li, M. and Yuan, Y. (2009). Joint regression analysis of correlated data using gaussian copulas. *Biometrics* **65**, 60-68.

Tsukahara, H. (2005). Semiparametric estimation in copula models. *Canad. J. Statist.* **33**, 357-375.

Wu, W. and Pourahmadi, M. (2003). Nonparametric estimation of large covariance matrices of longitudinal data. *Biometrika* **90**, 831-844.

Xue, L. and Zou, H. (2011). On optimal estimation of sparse correlation matrices of semiparametric Gaussian copulas. Technical Report, School of Statistics, University of Minnesota.

Xue, L. and Zou, H. (2012). Regularized rank-based estimation of high-dimensional nonparanormal graphical models. *Ann. Statist.*, **40**, 2541-2571.

Xue, L. and Zou, H. (2013). Minimax optimal estimation of general bandable covariance matrices. *J. Multivariate Anal.* **116**, 45-51.

Department of Statistics, The Pennsylvania State University, University Park, PA 16802, USA.

E-mail: lzxue@psu.edu

School of Statistics, University of Minnesota, Minneapolis, MN 55455, USA.

E-mail: zouxx019@umn.edu

(Received February 2012; accepted November 2012)